Correlations between communicability sequence entropy and transport performance in spatially embedded networks

Dan Chen, Rui-Wu Niu, and Gui-Jun Pan*
Faculty of Physics and Electronic Science, Hubei University, Wuhan 430062, China

(Received 19 December 2018; revised manuscript received 20 May 2019; published 24 June 2019)

We investigate electric current transport performances in spatially embedded networks with total cost restriction introduced by Li *et al.* [Phys. Rev. Lett. **104**, 018701 (2010)]. Precisely, the network is built from a d-dimensional regular lattice to be improved by adding long-range connections with probability $P_{ij} \sim r_{ij}^{-\alpha}$, where r_{ij} is the Manhattan distance between sites i and j, and α is a variable exponent, the total length of the long-range connections is restricted. In addition, each link has a local conductance given by $g_{ij} \sim r_{ij}^{-C}$, where the exponent C is to measure the impact of long-range connections on network flow. By calculating mean effective conductance of the network for different exponent α, we find that the optimal electric current transport conditions are obtained with $\alpha_{\text{opt}} = d + 1$ for all C. Interestingly, the optimal transportation condition is identical to the one obtained for optimal navigation in spatially embedded networks with total cost constraint. In addition, the phenomenon can be possibly explained by the communicability sequence entropy; we find that when $\alpha = d + 1$, the spatial network with total cost constraint can obtain the maximum communicability sequence entropy. The results show that the transport performance is strongly correlated with the communicability sequence entropy, which can provide an effective strategy for designing a power network with high transmission efficiency, that is, the transport performance can be optimized by improving the communicability sequence entropy of the network.

DOI: 10.1103/PhysRevE.99.062310

I. INTRODUCTION

The relation between network structure and function is determinant for the behavior of complex systems based on networks. A fundamental question at the core of the relationship is the properties of the networks that optimize the dynamics with respect to a given performance measure. For more than ten years, there has been a lot of research on this topic in a wide range of contexts, such as synchronization [1,2], diffusion dynamics [3,4], dynamical stability [5], and controllability [6]. Especially, the transport of information and energy in the network can be optimized by adding long-range connections (shortcuts) to an underlying geographical network [7–12]. This implies that reasonable design network can make information flow efficiently from source to target in the geographical network.

For concreteness, Kleinberg has studied the optimal navigation with local knowledge by adding the long-range connections to a d-dimensional lattice [7], where each node is connected with its neighbors and randomly generates a long-range connection with a probability $P_{ij} \sim r_{ij}^{-\alpha}$, where r_{ij} is the Manhattan distance between sites i and j, and α is a variable exponent, these results indicate that the small-world features of the network can only be efficiently accessed if the exponent is precisely set at $\alpha = d$. Roberson *et al.* studied the navigation problem in fractal small-world networks [8], and they proved that $\alpha = d$ is also the optimal power-law exponent in the fractal case. Hu *et al.* used the entropy concept of statistical physics to prove that the PDF of the distance from a given node is $p(r) \propto r^{-1}$ for all d, the network structure is optimal for navigation [13]. In fact, transport is usually constrained by some involved cost [10–12]. Based on this idea, Li *et al.* proposed a cost constraint on the total length of the additional links [10,11]. They found an interesting phenomenon that the optimal transport condition is obtained with a power-law exponent $\alpha = d + 1$ for both local and global navigation. Recently, Niu *et al.* [14] investigated random walk with a bias toward a target node in Li networks, the bias is represented by the parameter p, which is the probability that the packet follows the greedy algorithm for navigation, they found the best transportation condition is obtained with an exponent $\alpha = d + 1$ for all p.

Recently, to explore how efficient small-world networks are for transport phenomena that typically obey local conservation laws, Oliveira *et al.* [15] studied the enhanced flow properties in Kleinberg spatial networks, by considering that each link has a local conductance given by $g_{ij} \sim r_{ij}^{-C}$, where the exponent C is to measure the impact of long-range connections on network flow. Similar to the effective navigation in the network, they have shown that enhanced flow properties can also be observed in these small-world topologies. That is, the best flow conditions are obtained for $C = 0$ with $\alpha = 0$; for $C \approx 1$, the optimal condition is obtained at $\alpha = d$. And the optimal condition is identical to the one obtained for optimal navigation in small-world networks using decentralized algorithms.

To explore the effects of the cost constraint on the electric current transport performance of the spatially embedded networks, in this paper, we study current transport characteristics in spatially embedded networks with total cost restriction by considering that the local conductance of each link is given by

*pangj8866@hubu.edu.cn

 ©2019 American Physical Society

$g_{ij} \sim r_{ij}^{-C}$. Our results show that the optimal current transport condition is obtained with $\alpha = d + 1$. It is worth noting that this condition does not seem to change for different regulatory parameters C. In particularly, the optimal condition is identical to the one obtained for optimal navigation in spatially embedded networks with total cost constraint for both local and global knowledge [10,11].

Furthermore, by using the theoretical tool of describing the communicability between network nodes proposed by Estrada *et al.* [16–19], we have recently proposed the communicability sequence entropy of network that can effectively reflect the global information of the network, and on the basis of this entropy measure, the Jensen-Shannon divergence of two networks can be used to accurately compare the differences between networks [20]. Here, we further discuss the relations between communicability sequence entropy and the spatial structure of the network, and our results show that, when $\alpha = d + 1$, the spatial network with total cost constraint can obtain the maximum communicability sequence entropy. That is, the transport performance is optimal when the communicability sequence entropy reaches the maximum, which indicates that the transport performance is strongly correlated with communicability sequence entropy.

The paper is organized as follows. In Sec. II we describe in detail the generation steps of the spatially embedded network model and the corresponding dynamic model. In Sec. III we investigate electric current transport performances in spatially embedded networks with total cost constraint. Then we show that the phenomenon can be possibly explained by the communicability sequence entropy.

II. NETWORK AND TRANSPORT MODELS

A. Spatially embedded network model

There are many long-range connections in spatially embedded networks, and often the distribution of the link lengths r follows a power law, $p(r) \sim r^{-u}$ [21]. In addition, for some spatially embedded networks, the total length of long-range connections is subject to cost constraints. Based on the structural characteristics of these real networks, Li *et al.* [10,11] proposed a spatially embedded network model where a cost constraint on the total length of the additional links is imposed. The model can be described as follows:

The network model consists of $N = L^d$ nodes arranged d-dimensional regular lattice, and each node is connected with its $2d$ nearest neighbors, pairs of nodes i and j are randomly chosen to receive long-range connections with probability, $P_{ij} \sim r_{ij}^{-\alpha}$, where r_{ij} is the Manhattan distance between nodes i and j, namely, shortest path between i and j. And the total length of the long-range connections is restricted by $\lambda = \Gamma N$, where Γ is a constant. The probability P_{ij} that nodes i and j will have a long-range connection can be mapped on a density distribution $p(r)$, where $r = r_{ij}$. Thus, the distance distribution of the long-range connections $p(r) \sim r^{-\alpha} r^{d-1}$ can be normalized as $\int_1^{r_{\max}} p(r)dr = 1$, from which

$$p(r) = \begin{cases} (d-\alpha)\frac{1}{(r_{\max})^{d-\alpha}-1} r^{-\alpha} r^{d-1}, & \alpha \neq d, \\ \frac{1}{\ln(r_{\max})} r^{-\alpha} r^{d-1}, & \alpha = d. \end{cases} \quad (1)$$

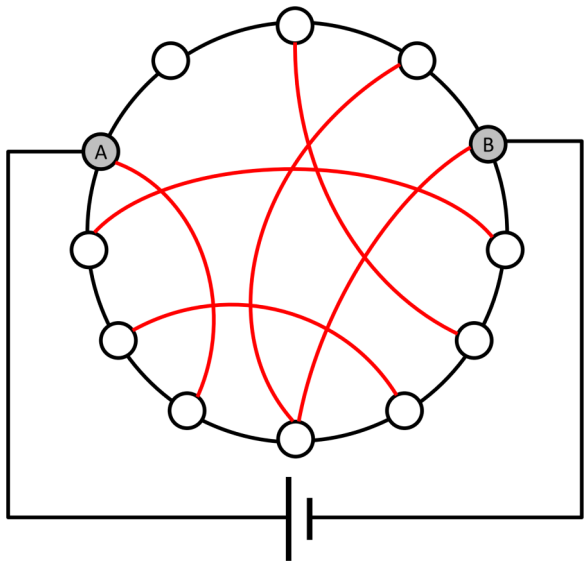

FIG. 1. The network is implemented by added long-range connections (in red) to a one-dimensional nearest-neighbor coupled network (nearest neighbor number $K = 2$). Each connection has a local conductance given by g_{ij}, a unitary global current is added between nodes A and B, then $G_{AB} = 1/(V_A - V_B)$. So the mean global conductance $\langle G \rangle$ is obtained by averaging over different pairs of nodes and different realizations of the network.

Here, $r_{\max}$ is the maximum distance between any two nodes in the original underlying regular lattice. When $d = 1$, $r_{\max} = L/2$, and when $d = 2$, $r_{\max} = L$. And then, the distance r can be obtained from random numbers $0 \leqslant \delta < 1$ chosen from the uniform distribution, by

$$r = \begin{cases} [1 - \delta(1 - (r_{\max})^{d-\alpha})]^{1/(d-\alpha)}, & \alpha \neq d, \\ (r_{\max})^{\delta}, & \alpha = d. \end{cases} \quad (2)$$

In this work, $d = 1$ and $d = 2$. The network model can be generated following algorithm in Refs. [10,11,14,21]:

(i) Creating a regular d-dimensional regular lattice with N nodes with each node connected to its $2d$ nearest neighbors.

(ii) We randomly chose a node i to create a long-range connection. The length of the long-range connection r ($1 < r \leqslant r_{\max}$) is randomly selected using Eqs. (2). We consider all N_r nodes on the Manhattan distance $S = [r]$ (if $r - [r] > 0.5$, then $S = [r] + 1$, and if $r - [r] \leqslant 0.5$, then $S = [r]$) from node i, that are not yet connected to node i.

(iii) We randomly select a node j from the N_r nodes and then connect nodes i and j.

(iv) Return to step (ii), until the total length of the long-connections reach the preset cost λ, e.g., $\lambda = \Gamma N$.

B. The electric current transport model

After the network has been built, we need the following additional settings for the current transport model. First, we associate each link to an Ohmic resistor. Second, select two nodes A and B, and add unitary global current between them. If we regard the whole network as a circuit, then A is the input node of the whole circuit and B is the output node (see Fig. 1). To compute the local potential V_i, we solve

Kirchhoff's law [22–26] at each site i,

$$\sum_j g_{ij}(V_i - V_j) = 0, \quad i = 1, \ldots, N. \tag{3}$$

Equation (3) [15] can be understood as the algebraic sum equal to 0 of currents on the branches directly connected to the node i, and g_{ij} being the link conductance between i and j. A pair of nodes A and B are selected as the current input and output in the network, the global conductance of the circuit depends on the potential difference between A and B, so $G \equiv 1/\Delta V$ for a given realization, where $\Delta V = V_A - V_B$. According to this way, the conductance G between any two nodes can be calculated. Therefore, the mean global conductance $\langle G \rangle$ is obtained by averaging over different pairs of nodes and different realizations of the network.

According to the knowledge in the circuit, the conductance is equal to the reciprocal of resistance. To study the electrical transport performance of the network, it is necessary to assign appropriate conductance to each long-range connection. For the conductance of long-range connections, a reasonable null-model is that all these links have the same conductance. By contrast in certain real-world applications, one would expect that the resistance increases linearly with length. A function that interpolates between these cases is the power law, so we can think of the conductance of a long-range connection as a power function of the Manhattan distance between two points [15],

$$g_{ij} = r_{ij}^{-C}. \tag{4}$$

The connection types in the network include short-range connection and long-range connection, while the introduction of exponent C is to measure the impact of long-range connections on network flow. This means that as C increases, the contribution of longer connections to network flow is attenuated. In fact, we can explain the mechanism of current transmission on the network in three cases, (i) for $C < 1$, preferential flow in a network should be implemented through long-range connections, (ii) for $C > 1$, preferential flow in a network should be implemented through short-range connections, and (iii) for $C = 1$, is known as Pouillet's law, the conductance of a long-range connection with Manhattan distance r is equivalent to an effective conductance of r short-range links in series, hence one should expect long-range links contributing to transport as much as short-range links [15].

III. RESULTS AND DISCUSSION

A. Transport on spatially embedded networks

First, we study the optimal electrical transport conditions for a one-dimensional spatially embedded network with total cost constraints. Figure 2 shows the distribution $P(GN)$ of local conductance for different α on a one-dimensional spatially embedded network with additional long-range connections of total length $\lambda = 10N$, where GN represents the product of local conductance and network size. In Fig. 2(a), when $C = 0$, $P(GN)$ follows an approximate Gaussian distribution for $\alpha = 1$ and $\alpha = 2$, and we can clearly see that the average conductance $\langle G \rangle$ can obtain the maximum value when $\alpha = 2$. For $C = 1$, $P(GN)$ is approximately subject to a power-law distribution, as shown in Fig. 2(b), and we can roughly

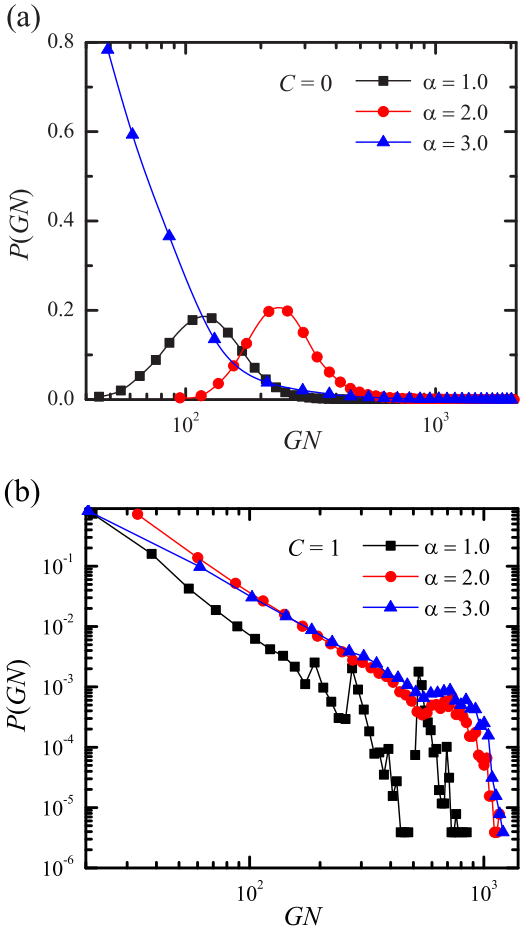

FIG. 2. Local conductance probability distribution for each connection of a one-dimensional embedded network, where the total length is limited to $\lambda = 10N$, $N = 512$. (a) $C = 0$ and (b) $C = 1$. We sampled $500N$ realizations for each α.

evaluate the maximum average conductance to be obtained at $\alpha = 2$.

In Figs. 3(a) and 3(b) we show the dependence of mean effective conductance $\langle G \rangle$ of one-dimensional spatially embedded networks with total cost constraints on network parameters α and N. In all networks, the total length λ of the added long-range connections are limited to $10N$. As shown in Fig. 3(a), for all different sizes of networks, the network conductance $\langle G \rangle$ decays nonmonotonically with α for $C = 0$, that is, the mean effective conductance $\langle G \rangle$ increases with the increase of α, and then decreases gradually. Here, we find that when N is high (such as $N \geqslant 512$), the maximum mean effective conductance $\langle G \rangle$ is obtained at $\alpha_{\text{opt}} = 2$, and for sufficiently large parameter α, the average conductance $\langle G \rangle$ is almost constant. Similarly, in Fig. 3(b) we show the dependence of mean effective conductance $\langle G \rangle$ on the parameter α for $C = 1$, a similar conclusion has been obtained, we find that when N is high, the maximum mean effective conductance $\langle G \rangle$ is also obtained at $\alpha_{\text{opt}} = 2$. In fact, we know that the local conductance between any two nodes at $C = 0$ is independent of the distance, which means that the long-range connections and the short-range connections correspond to the same conductance. However, for $C = 1$, the local conductance

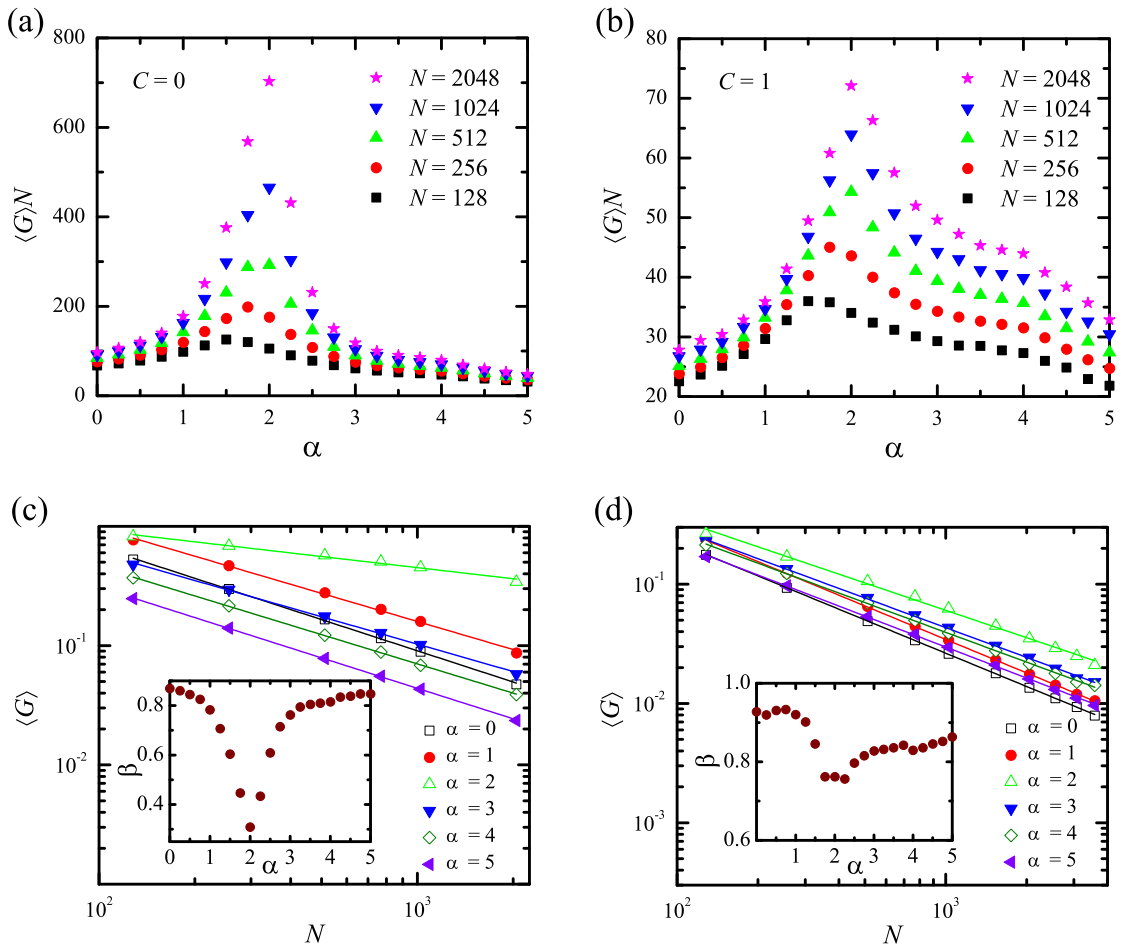

FIG. 3. Dependence of mean effective conductance $\langle G\rangle$ of one-dimensional spatially embedded networks with total cost constraints on network parameters (α and N). For $C = 0$, in (a) we show the relationship between $\langle G\rangle$ and the control parameter α, for large N, the maximum conductance is obtained at $\alpha_{\rm opt} = 2$, and in (b) we show the case of $C = 1$. In (c) and (d) we show the dependence of mean effective conductance $\langle G\rangle$ on the network size N for $C = 0$ and $C = 1$. The average conductance always obeys a power law behavior $\langle G\rangle \sim N^{-\beta}$ for different values of α. The inset shows the relationship between exponent β and α. The total length λ of the added long-range connections is limited to $10N$. The results are averaged $5000N$ realizations for $N = 128$ and $N = 256$, $500N$ realizations for $N = 512$, $250N$ realizations for $N = 1024$, and $50N$ realizations for $N = 2048$.

of the long-range connection is less than the local conductance of the short-range connection. Therefore, under the same conditions, the mean effective conductance at $C = 0$ is greater than the mean effective conductance at $C = 1$.

In Figs. 3(c) and 3(d) we show the dependence of the mean effective conductance on the network size N for $C = 0$ and $C = 1$. The results indicate that the exponent α is varied from 0 to 5, the average conductance always obeys a power-law behavior $\langle G\rangle \sim N^{-\beta}$, and the inset shows the relationship between the exponent β and α. Our results show that, for $\alpha < 2$, the exponent β decreases with the increase of α, for $\alpha > 2$, β increases with the increase of α. In particular, the minimum value of β is obtained at $\alpha_{\rm opt} \approx 2$. For $C = 0$, the minimum value of β is clearly obtained at $\alpha_{\rm opt} = 2$. These results reflect the following fact that, under the optimal conditions, the transport performance of the network decline at the slowest speed with the increase of size.

Next, we study the optimal electrical transport conditions for a two-dimensional spatially embedded network with total cost constraints, namely, the network is built form $N = L \times L$ square lattices to be improved by adding long-range connections. Figure. 4(a) shows the dependence of average conductance on parameter α for $L = 50$ and $L = 100$, where $C = 0$ and $\lambda = N$. In this case all links have identical local conductances, the maximum mean conductance is obtained at $\alpha = 3$. For $C = 1$, the local conductance of each connection is inversely proportional to the link length. For $L = 50$, the maximum values of the average conductance is obtained at $\alpha_{\rm opt} \approx 3.9$, and for $L = 100$, $\alpha_{\rm opt} \approx 3.5$. In addition, $\alpha_{\rm opt}$ decreases with the increase of L, the inset of Fig. 4(b) shows the relationship between $\alpha_{\rm opt}$ and L^{-1}. We find that $\alpha_{\rm opt}$ and L^{-1} are approximately subject to linear relations, and the result of linear fitting is $\alpha_{\rm opt} = 3.086 + 40.228L^{-1}$. So, when $L \to \infty$, $\alpha_{\rm opt} \approx 3 = d + 1$.

The parameter C is introduced to measure the impact of the long-range connections on the network global flow. For $C = 1$ and $C = 0$, the maximum conductance values are obtained at $\alpha_{\rm opt} = d + 1$. Finally, to explore more detailed current transport characteristics in the network. We investigate the dependence of the mean global conductance on the parameter

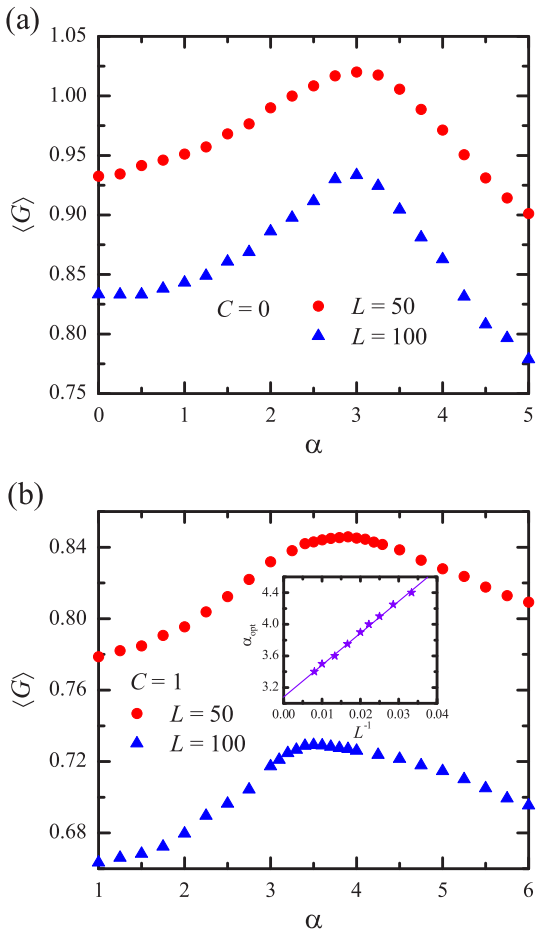

FIG. 4. We show the dependence on α of the average conductance of the network is built form $N = L \times L$ square lattices to be improved by adding long-range connections. In (a), the maximum values of the average conductance are obtained at $\alpha_{\text{opt}} \approx 3$ for $C = 0$. In (b) the maximum values of the average conductance are obtained at $\alpha_{\text{opt}} \approx 3.9$ for $L = 50$, and at $\alpha_{\text{opt}} \approx 3.5$ for $L = 100$. The inset shows the dependence of α_{opt} on L^{-1}, the result of linear fitting is $\alpha_{\text{opt}} = 3.086 + 40.228L^{-1}$.

C for one-dimensional spatially embedded networks with total cost constraints. As shown in Fig. 5, the exponent C is varied from 0 to 2. We find that when the exponent α is given a fixed value, the average effective conductance decreases with the increase of C. The reason is that, with the increase of C, the contribution of longer connections to flow is gradually diminishes. Most importantly, the maximum effective conductance values are obtained at $\alpha_{\text{opt}} = d + 1$ for all C. For $0 \leqslant C \leqslant 1$, this phenomenon is more obvious, for $1 \ll C \leqslant 2$, when α is more than 2, the conductance decreases very slowly with the increase of α, and almost remains unchanged.

B. Communicability sequence entropy of spatially embedded networks

According to Kirchhoff's law, we can find that the conductance between any pair of nodes in the network takes all possible circulation circuits into consideration. Similarly, in a complex network, the communicability between any pair of nodes p and q in a network is the weighted sum of all walks

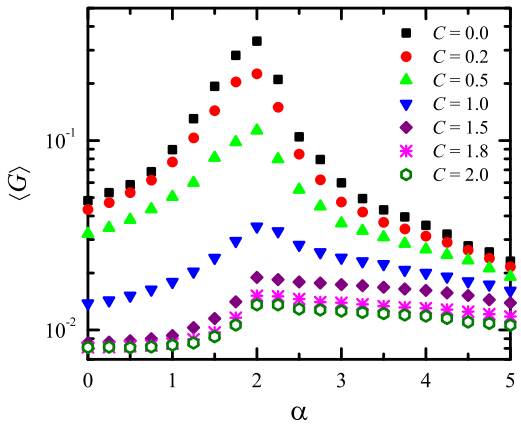

FIG. 5. We show the dependence on α of the mean effective conductance of the network for different values of C. The underlying substrate is an one-dimensional spatially embedded network with total cost constraints ($N = 2048$, $\lambda = 10N$). The optimal global conductance is obtained at $\alpha_{\text{opt}} = 2$ for all C. The results are averaged $1000N$ realizations.

starting at node p and ending at node q, in which the weighting scheme gives more weight to the shortest walks than to the longer ones [16]. This seems to imply that there may be some correlation between the network's electrical transport performance and communicability. In Ref. [20], we have found that the overall communicability characteristics of the network can be represented by the communicability sequence entropy, so there maybe have some correlations between the communicability sequence entropy and the electrical transport performance of the network. To this end, we will study the communicability sequence entropy of spatially embedded networks and further explore the correlation between it and electrical transport performance.

We consider an unweighted and undirected network with N nodes and E edges, where the connected edges between nodes are represented by the $N \times N$ adjacency matrix A. The matrix A describes the connection between nodes in a network; if node i is directly connected to node j, then $A_{ij} = 1$, otherwise $A_{ij} = 0$. To measure the communicability between nodes in the network, a communicability network matrix is proposed in Ref. [16],

$$G^{\text{EA}} = e^{A} = \sum_{k=0}^{\infty} \frac{1}{k!} A^{k} = \begin{Bmatrix} G_{11}^{\text{EA}} & G_{12}^{\text{EA}} & \cdots & G_{1N}^{\text{EA}} \\ G_{21}^{\text{EA}} & G_{22}^{\text{EA}} & \cdots & G_{2N}^{\text{EA}} \\ \vdots & \vdots & \ddots & \vdots \\ G_{N1}^{\text{EA}} & G_{N2}^{\text{EA}} & \cdots & G_{NN}^{\text{EA}} \end{Bmatrix}. \tag{5}$$

The communicability between the nodes i and j is the element corresponding to the i row j column of the matrix G^{EA}: G_{ij}^{EA}. The G_{ij}^{EA} effectively takes into account all possible paths between the nodes i and j, and can provide quantitative measures of correlation and information flow between different parts of a network [16–19]. Using the eigendecomposition of the adjacency matrix $A = Q\Lambda Q^{-1}$, $e^{A} = Qe^{\Lambda}Q^{-1}$, $\Lambda = \text{diag}[\lambda_1(A), \lambda_2(A), \cdots \lambda_k(A), \cdots, \lambda_N(A)]$, where $\lambda_k(A)$ indicates the kth eigenvalue of A, and Q is an orthogonal

matrix consisting of a corresponding standard orthogonal basis.

To measure the influence of long-range connections on network's communicability, by analogy to Eq. (4), let us consider the weighted matrix W of the adjacency matrix A, where

$$W_{ij} = \begin{cases} r_{ij}^{-C}, & \text{if } A_{ij} = 1, \\ 0, & \text{if } A_{ij} = 0. \end{cases} \tag{6}$$

Correspondingly, the communicability matrix is

$$G^{\mathrm{EW}} = e^{W}. \tag{7}$$

The above processing is based on the assumption that the communicability between two nodes will decline with the increase of the edge length. In fact, when $C = 0$, $W = A$, $G^{\mathrm{EW}} = G^{\mathrm{EA}}$.

We store the elements $G_{ij}^{\mathrm{EW}}(i < j)$ in a set σ, and the sum of all the elements of the collection of σ is $\Sigma = \sum_{i<j} G_{ij}^{\mathrm{EW}}$. So we can get the normalized sequence $P = \{P_1, P_2, \ldots, P_k, \ldots, P_M\}$ by σ, where $P_k = G_{ij}^{\mathrm{EW}}/\Sigma$, $(1 \leqslant k \leqslant M, 1 \leqslant i < j \leqslant N)$, $M = N(N-1)/2$, and $\sum_{k=1}^{M} P_k = 1$. We call P the communicability sequence of the network. The Shannon entropy of the sequence is expressed as

$$S(P) = -\sum_{i=1}^{M} P_i \log_2 P_i; \tag{8}$$

we call $S(P)$ as the communicability sequence entropy of the network, where by convention $0 \log_2 0 := 0$. To eliminate the effects of network size, we define the normalized entropy to be

$$S_N = \frac{1}{\log_2 M} S(P). \tag{9}$$

The results of Ref. [15] show that when $C = 0$, the best transport conditions are obtained at $\alpha_{\mathrm{opt}} = 0$, and when $C = 1$, the best transport conditions are obtained at $\alpha_{\mathrm{opt}} = d$. For the Kleinberg model, the smaller α corresponds to more long-range connections, and the larger α corresponds to more short-range connections, i.e., the total cost of the network is different for different α. In this paper, we limit the total cost, and the results show that for different C, the best transport conditions are obtained at $\alpha_{\mathrm{opt}} = d + 1$. Now, we will focus on the possible causes behind this. The concept of entropy will be used here to explain, but the forms of entropy are varied, so choosing a suitable entropy is undoubtedly crucial. In the previous work, we extracted a kind of communicability sequence entropy from the communicability between network nodes, which can represent the global communicability of the network and can also be used to quantify the difference between networks [20].

Next, we investigate the communicability sequence entropy for one and two-dimensional spatially embedded network with total cost restriction. Figure 6 shows the dependence of the normalized entropy S_N on the parameter α. In Figs. 6(a) and 6(b), for $C = 0$ and $C = 1$, S_N increases gradually and then decreases gradually with the increase of α. When the network size is large enough, the maximum point is finally stable around $\alpha = 2$, this is consistent with the optimal flow conditions observed in Figs. 3(a) and 3(b). For $d = 2$ and $C = 0$, S_N presented a similar change trend, the maximum point finally stable around $\alpha = 3$ [see Fig. 6(c)]. For $C = 1$, the maximum values of the S_N are obtained at $\alpha_{\mathrm{opt}} \approx 3.8$ for $L = 50$, and at $\alpha_{\mathrm{opt}} \approx 3.6$ for $L = 70$ [see Fig. 6(d)], the approximate linear fitting result is $\alpha_{\mathrm{opt}} = 3.1 + 35L^{-1}$. It is reasonable that we conjecture $\alpha_{\mathrm{opt}} \to 3$ when considering large enough system size and a sufficient number of statistical samples.

In fact, when the cost of adding long-range connections to the underlying network is constrained, it has been found that the optimal navigation conditions are obtained at $\alpha_{\mathrm{opt}} = d + 1$ [10,11], that is, the average shortest path length is the minimum. The results of this paper show that the network has the best electrical transport condition at $\alpha_{\mathrm{opt}} = d + 1$, which to some extent reflects another excellent performance of the spatially embedded network when $\alpha = d + 1$. The above results indicate that S_N gets the maximum at $\alpha_{\mathrm{opt}} = d + 1$. Therefore, for a spatially embedded network with total cost constraint, the higher S_N is, the better the network's transport performance is. In addition, the size of S_N reflects the uniformity of communicability between any pair of nodes in the network. Hence, the network's electrical transport performance and the uniformity of communicability sequence has a strong correlation.

To further illustrate whether this strong correlation property is common in spatially embedded networks or not, we also investigate the normalized entropy for two-dimensional Kleinberg network [7]. For $C = 0$, the weight of each edge is independent of the length, the maximum value of S_N is obtained at $\alpha_{\mathrm{opt}} = 0$, as shown in Fig. 7(a). Which is consistent with the optimal flow condition in the literature [15], and also identical to the optimal condition for navigating with global knowledge [27,28]. In addition, since each node will receive a long-range connection, and it is known from Eq. (2) that when $\alpha = 0$, almost every long-range connection connects two points far from each other in the underlying network, the communicability between all nodes is almost equal. So the communicability sequence entropy is maximum. For $C = 1$, the communicability of long-range connection between two nodes will be attenuated with the increase of weight (the length of the long-range connections). The maximum value of S_N is obtained at $\alpha_{\mathrm{opt}} = 2$, as can be seen from the Fig. 7(b). Furthermore, it is identical to the best flow conditions in the literature [15], and it is identical to the one obtained for navigating with local knowledge [7].

It is worth noting that in the navigation of the Kleinberg network, the optimal navigation conditions based on global knowledge and local knowledge are different, the former is $\alpha_{\mathrm{opt}} = 0$ [27,28], the latter is $\alpha_{\mathrm{opt}} = d$ [7]. For the transport capacity of the Kleinberg network, when the parameters $C = 0$ and $C = 1$, the optimal conditions for electric transport are $\alpha_{\mathrm{opt}} = 0$ and $\alpha_{\mathrm{opt}} = d$ [15], respectively. In other words, the optimal network structure parameter α is related to the dynamic parameter. Our research shows that for different dynamic parameters, the system's dynamic performance is optimal when the maximum communicability sequence entropy is obtained. These results show that it is universal to use communicability sequence entropy to characterize the optimal state of the system. However, the parameter α is a unique structural parameter of a spatially embedded network with

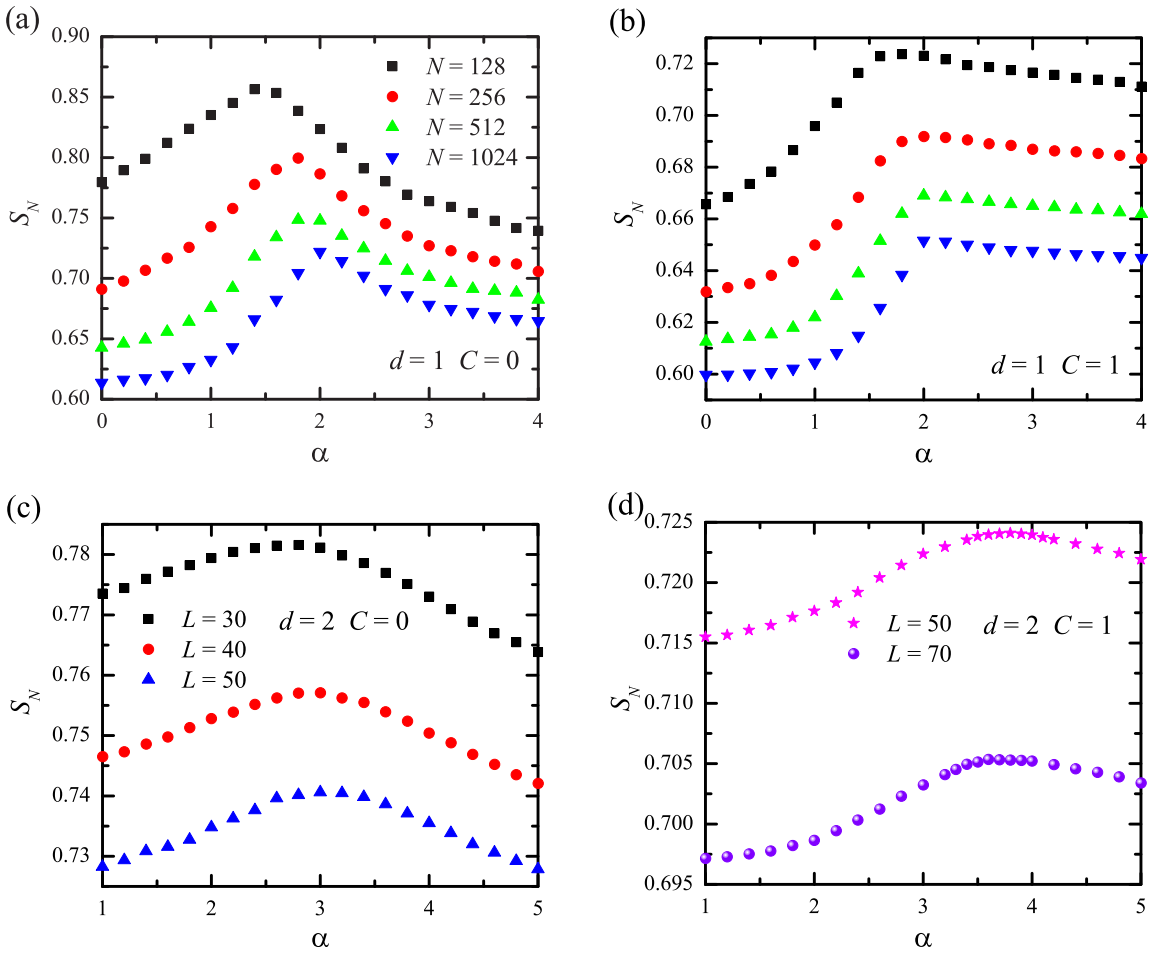

FIG. 6. Communicability sequence entropy of spatially embedded networks with total cost restriction. The normalized entropy S_N as a function of α for one- and two-dimensional spatially embedded networks, the total length λ of the added long-range connections is limited to $10N$ for the one-dimensional lattice, and N for the two-dimensional lattice. In (a) $d = 1, C = 0$ and (b) $d = 1, C = 1$, the maximum normalized entropy is obtained at $\alpha_{\text{opt}} = 2$. For $d = 2$, when $C = 0$, the maximum normalized entropy is obtained at $\alpha_{\text{opt}} = 3$. When $C = 1$, the maximum values of the normalized entropy are obtained at $\alpha_{\text{opt}} \approx 3.8$ for $L = 50$, and at $\alpha_{\text{opt}} \approx 3.6$ for $L = 70$.

power-law links length distribution. And the communicability sequence entropy is a structural measure of every network. Compared with parameter α, it is more convenient and practical to use a universal structural parameter, communicability sequence entropy, to characterize the optimal electrical transport capacity of the network. Furthermore, for a specific

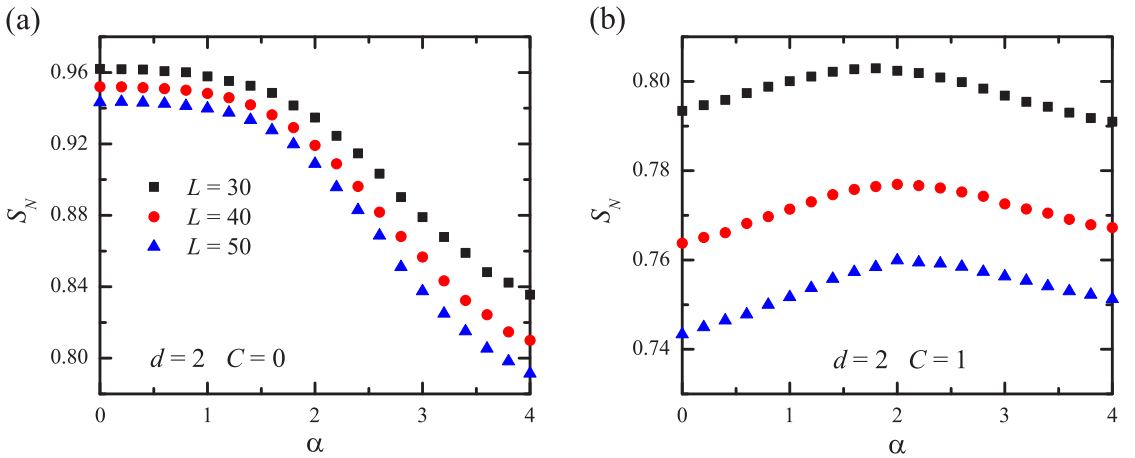

FIG. 7. The normalized entropy S_N as a function of α for two-dimensional Kleinberg networks. In (a) for $C = 0$, the maximum normalized entropy is obtained at $\alpha_{\text{opt}} = 0$. In (b) for $C = 1$, the maximum normalized entropy is obtained at $\alpha_{\text{opt}} = 2$.

power network, the communicability sequence entropy can be used to characterize the power transport performance. Therefore, a high transmission efficiency network can be designed by optimizing the communicability sequence entropy.

IV. CONCLUSIONS

We investigate electric current transport performances in spatially embedded networks with total cost restriction [10]. Our results showed in what conditions enhanced flow can be observed in spatially embedded networks with total cost constraint. The specific method is to assign a local conductance $g_{ij} \sim r_{ij}^{-C}$ to each link and then calculate the mean effective conductance of the network, when the conductance reaches the maximum, the network will obtain the optimal transport properties. We study the relationship between the mean effective conductance $\langle G \rangle$ and α for different system sizes. Our results show that, when an appropriate total length λ of the added long-range connection is considered, the optimal current transport condition is obtained with $\alpha_{\text{opt}} = d + 1$ for all C. In addition, we show the dependence of the mean effective conductance on the network size N for $C = 1$ and $C = 0$. The results indicate that, the average conductance always obeys a power-law behavior $\langle G \rangle \sim N^{-\beta}$, and the minimum value of β is obtained at $\alpha_{\text{opt}} = d + 1$. In particular, this exponent is identical to the one obtained for optimal navigation in spatially embedded networks with total cost constraint for both local and global knowledge [10,11].

In addition, we propose a measure to characterize the global communicability of the network: communicability sequence entropy. We find that, for spatially embedded networks with total cost constraints, when $C = 0$ and $C = 1$, the communicability sequence entropy S_N reaches the maximum at $\alpha_{\text{opt}} = d + 1$. For Kleinberg networks, when $C = 0$, the maximum S_N is obtained at $\alpha_{\text{opt}} = 0$, and when $C = 1$, the maximum S_N is obtained at $\alpha_{\text{opt}} = d$. The results show that the transport performance is strongly correlated with the communicability sequence entropy, which can provide an effective strategy for designing a power network with high transmission efficiency. Finally, according to the results of this paper, the communicability sequence entropy can be used to characterize the dynamic performance of spatially embedded networks. However, for other networks without spatial structure have such characteristics is still unknown. Therefore, these issues need to be further explored in future work.

ACKNOWLEDGMENTS

This work was supported by the Education Foundation of Hubei Province through Grant No. (D20120104). We thank the two referees for their valuable comments, which have played an important role in improving the quality of the paper and benefited us a lot.

[1] S. Boccaletti, V. Latora, Y. Moreno, M. Chavez, and D. U. Hwang, Phys. Rep. **424**, 175 (2006).
[2] M. Barthélemy, Phys. Rep. **499**, 1 (2011).
[3] R. Cohen and S. Havlin, *Complex Networks: Structure, Robustness and Function* (Cambridge University Press, Cambridge, 2010).
[4] M. E. J. Newman, *Networks: An Introduction* (Oxford University Press, Oxford, 2010).
[5] A. Pomerance, E. Ott, M. Girvan, and W. Losert, Proc. Natl. Acad. Sci. USA **106**, 8209 (2009).
[6] A. J. Whalen, S. N. Brennan, T. D. Sauer, and S. J. Schiff, Phys. Rev. X **5**, 011005 (2015).
[7] J. M. Kleinberg, Nature (London) **406**, 845 (2000).
[8] M. R. Roberson and D. ben-Avraham, Phys. Rev. E **74**, 017101 (2006).
[9] L. Daqing, K. Kosmidis, A. Bunde, and S. Havlin, Nat. Phys. **7**, 481 (2011).
[10] G. Li, S. D. S. Reis, A. A. Moreira, S. Havlin, H. E. Stanley, and J. S. Andrade, Phys. Rev. Lett. **104**, 018701 (2010).
[11] G. Li, S. D. S. Reis, A. A. Moreira, S. Havlin, H. E. Stanley, and J. S. Andrade, Phys. Rev. E **87**, 042810 (2013).
[12] Q. Chen, J.-H. Qian, L. Zhu, and D.-D. Han, Phys. Rev. E **93**, 032321 (2016).
[13] Y. Hu, Y. Wang, D. Li, S. Havlin, and Z. Di, Phys. Rev. Lett. **106**, 108701 (2011).
[14] R.-W. Niu and G.-J. Pan, Physica A **461**, 9 (2016).
[15] C. L. N. Oliveira, P. A. Morais, A. A. Moreira, and J. S. Andrade, Phys. Rev. Lett. **112**, 148701 (2014).
[16] E. Estrada, N. Hatano, and M. Benzi, Phys. Rep. **514**, 89 (2012).
[17] E. Estrada and Jesús Gómez-Gardeñes, Phys. Rev. E **89**, 042819 (2014).
[18] E. Estrada, Phys. Rev. E **88**, 042811 (2013).
[19] E. Estrada and N. Hatano, Phys. Rev. E **77**, 036111 (2008).
[20] D. Chen, D.-D. Shi, M. Qin, S.-M. Xu, and G.-J. Pan, Phys. Rev. E **98**, 012319 (2018).
[21] T. Emmerich, A. Bunde, S. Havlin, G. Li, and D. Li, Phys. Rev. E **87**, 032802 (2013).
[22] M. E. J. Newman and M. Girvan, Phys. Rev. E **69**, 026113 (2004).
[23] F. Wu and B. A. Huberman, Eur. Phys. J. B **38**, 331 (2004).
[24] E. López, S. V. Buldyrev, S. Havlin, and H. E. Stanley, Phys. Rev. Lett. **94**, 248701 (2005).
[25] G. Korniss, M. B. Hastings, K. E. Bassler, M. J. Berryman, B. Kozma, and D. Abbott, Phys. Lett. A **350**, 324 (2006).
[26] The resulting systems of linear algebraic equations were solved through the HSL library, a collection of FORTRAN codes for large-scale scientific computation. See http://www.hsl.rl.ac.uk/.
[27] C. F. Moukarzel and M. Argollo de Menezes, Phys. Rev. E **65**, 056709 (2002).
[28] K. Kosmidis, S. Havlin, and A. Bunde, Europhys. Lett. **82**, 48005 (2008).